Fire testing and mechanical properties of neat and elastomeric polylactic acid composites reinforced with raw and enzymatically treated hemp fibers

Antoine Gallos, Océane Lannoy, Séverine Bellayer, Gaëlle Fontaine, Serge Bourbigot & Florent Allais

Published online: 12 Jan 2023.

Submit your article to this journal ↗

Article views: 423

View related articles ↗

View Crossmark data ↗

Taylor & Francis
Taylor & Francis Group

🔓 OPEN ACCESS | Check for updates

Fire testing and mechanical properties of neat and elastomeric polylactic acid composites reinforced with raw and enzymatically treated hemp fibers

Antoine Gallos[a], Océane Lannoy[a,b], Séverine Bellayer[b], Gaëlle Fontaine[b], Serge Bourbigot[b,c] and Florent Allais[a]

[a]URD Agro-Biotechnologies Industrielles (ABI), CEBB, AgroParisTech, Pomacle, France; [b]Univ. Lille, CNRS, INRAE, Centrale Lille, UMET – Unité Matériaux Et Transformations, Lille, France; [c]Institut Universitaire de France (IUF), Paris, France

ABSTRACT

A new class of biobased composites with tailorable mechanical properties made of natural fibers, polylactic acid, and ferulic acid derivatives (FAD) is studied. FAD was used to develop composites with elastomeric properties like improved elongation at break and highly reversible deformation upon elongation. Composites were prepared using raw and enzymatically treated hemp fibers. The fibers were defibrillated due to the enzymatic treatment increasing their aspect ratio. The composites were characterized by their mechanical properties and their reaction to fire. No significant change in the dispersion of the fibers in the composites was reported. Homogenously dispersed crystallites of FAD were observed by scanning electron microscopy in the PLA matrix and at the interface between the PLA and the fibers, where they are suspected to increase the free volume in correlation with a decrease in mechanical properties following the increase in the aspect ratio of the fibers. FAD also degraded the reaction to fire of the material with an increase in 10% of the peak of Heat Release Rate (pHRR) in comparison to neat PLA. It also increased the charring residue up to 3 wt.%. A synergistic effect between FAD and the lignin increasing the charring residue is also reported.
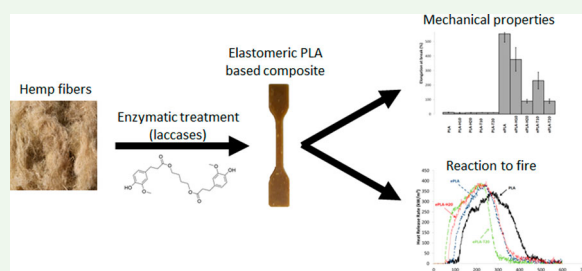
Introduction

Over the last decades plant fibers are much more considered to serve as reinforcement material especially since they are sustainable with high availability (*1*). Indeed, natural fibers can be produced from various plants all around the world (e.g. hemp, flax, ramie, jute, cotton, sisal, coir, bagasse, banana, pineapple, and wood). Composite materials find their uses in many applications (e.g. transportation, building, goods, and additive manufacturing) and their markets are growing (*2*). As a consequence, thermoplastic polymers reinforced with natural fibers are preferred for applications requiring a good balance between costs, processability, and performance, (*1,3,4*) but these materials often encounter high flammability and poor reaction to fire, limiting their applications in some industrial sectors (e.g. building, transportation) (*5*). Nevertheless, end-of-life concerns account to favor of more sustainable composites. Indeed, LCA studies demonstrated the choice of the polymeric matrix is important regarding the sustainability of the resulting composites (*6*). To this aim, bio-based polymers, such as polylactic acid (PLA), are considered greener alternatives than oil-based polymers (e.g. polypropylene (PP)) (*7*). They also have a better perspective regarding end-of-life concerns (e.g. biodegradation, composting, and recycling) (*8,9*). Numerous works were conducted during the last decades to promote the use of PLA reinforced with natural fibers (*10–12*). These composites mainly exhibit high stiffness but low flexibility and elongation at

break reducing their interest for many uses. Elastomeric PLA could be a solution as elastomers reinforced with natural fibers have the potential to make stiff materials with relatively preserved elasticity and flexibility (13). Unfortunately, most of the published studies report the use of raw thermoplastic or plasticized PLA and no elastomeric PLA. Indeed, the literature report blends PLA and oil-based elastomers (e.g. thermoplastic polyurethane (TPU), natural rubber (NR)) suitable to serve for composite applications (14–18). The blends of PLA and natural rubber require coupling agents to solve compatibility problems and avoid defects in the material (14). Both NR and TPU exhibit end-of-life concerns due to poor recyclability and/or partial biodegradability (19–22). As an example, the market of coated fabric and alternatives to leather is in the urge for more recyclable soft materials to replace TPU (20,23).

Moreover, a surface treatment is often used on natural fibers to improve the surface adhesion between the fibers and the polymeric matrix (12,24,25). Chemical surface treatment and chemical grafting showed promising results in increasing the mechanical properties of composites. They also suffer from financial and environmental costs reducing their interest (25). Enzymatic treatments are more eco-friendly as the process requires less energy and they can be reused several times. Literature works were conducted on enzymatic grafting of ferulic acid on natural fibers to improve the mechanical properties of polypropylene (PP)-based composites (26).

Our previous works on the blending of a commercial grade of PLA with a significant amount of a ferulic acid derivative (hereafter named BDF) permitted the development of a material with an elastomeric behavior (27,28). Not only is ferulic acid, a naturally occurring compound (e.g. lignocellulosic biomass), but also BDF is synthesized through enzymatic catalysis. The plasticizing effect of BDF in PLA was investigated at a content up to 20 wt.% resulting in soften thermoplastic blends (29). The elastomeric behavior is obtained when an amount of 25 wt.% of BDF is incorporated in PLA and is optimal at 30 wt.% with an elongation at break higher than 400% (27,28). This fully bio-based elastomeric blend is hereafter named ePLA.

In this study, we reinforced ePLA with natural fibers to produce bio-based composites with a good balance between stiffness and elongation at break. The study aims to characterize the thermomechanical properties and the reaction to fire of composites of ePLA reinforced with non-treated or treated hemp fibers at different content from 10 to 20 wt.%. As discussed previously, the treatment of natural fibers is a common way to improve surface adhesion between the fibers and the polymeric matrix increasing mechanical properties (12). Grafting the ferulic acid derivatives at the surface of the hemp fibers should improve the interface between the fibers and the PLA matrix. The mechanical properties of bio-based composites are of great importance as they will determine their potential as replacement materials for less sustainable composites. Studying the reaction to fire is also interesting to investigate the potential for applications in industrial sectors (e.g. furniture, building, and transportation). Moreover, the reaction to fire of blends of PLA and BDF was never studied before.

Hemp fibers were used in a will of valorizing the local natural resources. The hemp fibers were pretreated to enhance their aspect ratio and to increase the surface contact between the fibers and the polymer (4,12). The first step of this work was to pretreat the hemp fibers using an enzymatic process. The enzymatic treatment with laccase from Trametes Versicolor and BDF is in accordance with green chemistry principles and offers a soft pretreatment process. In the second step, non-treated and treated hemp fibers were incorporated into raw PLA or ePLA by the hot-melt process. The set of materials prepared with raw PLA was done as a reference to make comparisons between thermoplastic and elastomeric matrices. The resulting composites were characterized in the third step. Tensile testing was used to quantify the mechanical properties of the composites and to determine the effect of the matrix as well as that of the enzymatic treatment of the fibers. The aspect ratio and the surface of the fibers were investigated by Scanning Electron Microscopy (SEM) before and after the enzymatic treatments. The dispersion of the fibers was characterized by optical microscopy. The interface between the fibers and the PLA was observed by SEM. The thermal properties and the reaction to fire of the composites were analyzed by thermo-gravimetric analyses and cone calorimetry to investigate the synergistic effect between PLA, BDF, and fibers.

Experimental section

Materials

Composites were prepared with Ingeo PLA 4043D from NatureWorks. This PLA has a glass transition (Tg) from 55 to 60 °C and a melting point of 160 °C. It contains 4.3% of the D-lactide unit. Fibers Recherches Développement® (Troyes, France) provided hemp fibers (Cannabis sativa, variety Fedora 17, monoicous plants). These fibers were chopped into 5 mm-long pieces; they still contained some woody impurities. Ferulic acid (reagent grade, ≥99% purity) was purchased from Sigma-Aldrich. 1,4-Butanediol (reagent grade, 99%

purity) was purchased from Alfa Aesar. The BDF was prepared as described elsewhere (30,31). The enzyme (Laccase from Trametes Versicolor) was purchased from Novozyme.

Pretreatment of fibers

Two sets of composites were prepared. For the first set, fibers were incorporated into the polymer without any pretreatment. For the second set, fibers were pretreated with an enzymatic treatment involving Laccase and BDF before their incorporation into the PLA matrix. Each batch of treated fibers was prepared by the immersion of 11 g of crude fibers, 1.1 g of BDF (after being dissolved in 25 mL of acetone), and 110 mg of Laccase (1 mg ≥ 10 U) in a beaker containing 300 mL of a citrate/phosphate buffer (pH = 5.6). The dissolution in acetone was done to help the dispersion of BDF in water. The batch was then stirred at 600 RPM for 48 h at 40 °C. The beaker was not sealed during the enzymatic reaction as oxygen is required for the laccase to oxidize phenols (32). Under the experimental conditions, acetone was removed from water by evaporation as there is no azeotrope. The batch was then filtered and rinsed 3 times with 500 mL of water until the pH reached 7. The filtered fibers were then dried in an oven at 105 °C for 48 h. The mass was approximately 9.2 ± 0.2 g for each batch, meaning there is a loss of mass of almost $24 \pm 2\%$. Five batches were prepared to have a suitable amount of treated fibers to perform the process of the composites. The 5 batches were mixed and homogenized before the hot-melting process.

Processing of composites

The composites were prepared by melt blending on a Haake Rheomix from ThermoFisher Scientific. The temperature was set at 180 °C and the screw rotational speed was at 50 RPM. The composites prepared are listed in Table 1. For the composites with PLA matrix, the PLA

Table 1. Composites of PLA and/or ePLA filled with non-treated or pretreated hemp fibers.

Sample name	PLA (wt.%)	BDF (wt.%)	Non-treated hemp fibers (wt.%)	Treated hemp fibers (wt.%)
PLA	100	0	0	0
PLA-H10	90	0	10	0
PLA-H20	80	0	20	0
PLA-T10	90	0	0	10
PLA-T20	80	0	0	20
ePLA	70	30	0	0
ePLA-H10	63	27	10	0
ePLA-H20	56	24	20	0
ePLA-T10	63	27	0	10
ePLA-T20	56	24	0	20

was first introduced in the feeder for 5 min and the fibers were added for 10 min. For the composites with the ePLA matrix, the PLA was first introduced in the feeder for 5 min then the BDF was added for 15 min, and the fibers were added and mixed for 10 min (27). The PLA reference was melt blended solely for 15 min. PLA was first introduced for 5 min, then the BDF was added for 15 min to prepare the ePLA matrix.

Composites were injected into tensile test specimens according to ISO 527-2-5 A (length = 74.0 mm, center width = 4.1 mm, and thickness = 2.0 mm). The specimens were prepared by injection molding using a bench scale DSM Xplore micro injection mold IM 12. The processing temperature was set at 180 °C. The mold temperature was set at 45 °C for composites with the PLA matrix and room temperature for composites with the ePLA matrix. The injection pressure was set at 1.6×103 kN.m^{-2}. It was maintained for 30 s before the removal of each specimen.

Plate samples with dimensions of 50 mm × 50 mm × 3 mm used for reaction to fire were prepared with a Fontijne heating press with a pressure of 5×103 kN.m^{-2} for 5 min. The temperature was set at 180 °C. The plates were cooled at 40 °C under pressure before their removal. The duration of the cooling ramp was 15 min.

Mechanical characterizations

The tensile testing was performed according to ISO 527-2-5 A standard (room temperature = 20 °C and room humidity = 65% RH) with a Desktop Universal Tester from Testwell equipped with a 2 kN sensor (corresponding to the maximum force that the device can provide). The specimens were clamped with serrated wedges between two crossheads. The constant displacement rate of the moving crosshead was set at 10 mm.min-1. The strain was measured in the longitudinal direction with a nominal length of 20 mm. Five specimens were tested for each formulation on each test. The specimens were stored in a controlled environment for 24 h before the experiments. The values given hereafter are mean ± the standard deviation σ.

Scanning electron microscopy & optical microscopy

Scanning Electron Microscopy (SEM) images were taken using a JEOL JSM 7800F LV scanning electron microscope at 5 kV and 20 mm working distance. Before analyses, fibers were deposited on carbon tape and were carbon coated using a Bal-Tec SCD005 sputter coater. Fourteen pictures were collected for each set of fibers with a scale from 1 μm to 100 μm. Two pictures of

each collection were chosen according to their representativeness. SEM images were also taken on fractured composites to investigate the interface between the fibers and the polymeric matrix. Nine pictures were taken for each composite.

The samples were embedded into epoxy resin, polished with SiC polishing papers from grade 80 up to grade 4000, and analyzed with a Keyence VHX-7000 optical microscope. Three pictures were taken for each composite.

Thermal analysis

The Thermo-Gravimetric Analyses (TGA) were conducted on a TA Q500 from TA Instruments with a heating ramp of $10°C.min^{-1}$ from 50 °C to 500 °C under a nitrogen flow of 60 mL.min^{-1}. An isotherm of 30 min at 50 °C was done before the heating ramp. T5% and Tdmax respectively correspond to the temperatures where 5% mass loss was reached and where the maximum value was reached for the derivative of the mass loss curve. The derivative of the mass loss curve corresponds to the thermal degradation rate. The final residue corresponds to the residual mass at 500 °C.

The Differential Scanning Calorimetry (DSC) was performed on a TA Q20 from TA Instruments with a heating and a cooling ramp of 10 °C.min-1 between −80 and 200 °C. Each material was analyzed during two cycles. The first cycle allowed determining the crystallinity fraction (χ) using the melting enthalpy and erasing the thermal history. Tg was determined during the second cycle. The margin of error was assumed to be equivalent to the one measured with 5 replicates of PLA in our previous study as long as we use the same standards to perform calibrations regularly, the same device, and the same grade of PLA (*29*).

Reaction to fire

The reaction to fire was performed on a Fire Testing Technology (FTT) mass loss calorimeter device (ISO 13927) and Reduced Mass Loss Cone (R-MLC) experiments. The external heat flux was calibrated at 35 kW.m^{-2} with a distance of 25 mm using a methane flow varying from 0 to 6.7 mL.min^{-1} to determine the calibration curve. The distance of 25 mm corresponds to the distance between the heat flux and the surface of the samples that were placed on a ceramic sample holder after being wrapped in an aluminum foil. The samples were exposed horizontally under the heat flux. The ignition of the gases released by the samples was forced using a spark (which was removed right after the ignition). The temperature of the burnt and

unburnt gases was measured at the top of the chimney of the mass loss calorimeter. The temperature recorded was used to determine the heat released rate (HRR) expressed in kW.m^{-2} and the total heat released (THR). Three plates of each composite were burnt to ensure the repeatability of the results. The margin of error of experiments conducted with a mass loss calorimeter is generally estimated at 10%.

Results and discussion

Pretreatment and surface analysis of hemp fibers

The ferulic acid derivative – BDF – was used in the pretreatment process for two reasons. First, it has a suitable chemical structure to be oxidized by the laccase in the enzymatic reaction and potentially bind at the surface of the fibers. Second, the BDF located at the surface of the fibers (grafted or deposited) would have affinities with the BDF contained in the ePLA matrix. As the pretreatment medium was rinsed only with water and as the BDF is not soluble in water, one can suggest there is still some BDF residue at the surface of the fibers (grafted or not). A significant mass ($24 \pm 0.2\%$) of fibers and BDF was lost during the treatment of the fibers. The filtrate was cloudy and yellowish and contained a significant amount of visible but very small particles. One can observe that the fibers were qualitatively degraded. The combination of laccase and BDF could have plasticized the middle lamella of the hemp fibers, mainly composed of lignin and hemicelluloses (*33*). Such plasticization in combination with stirring would lead to defibrillation of the cellulose fibrils explaining the presence of small particles in the filtrate. The fibers were characterized by SEM before and after the enzymatic treatment. The results are shown in Figure 1. The surface analyses of raw hemp fiber are presented in Figure 1(a,b) and of treated hemp fibers in Figure 1(c, d). A partial defibrillation of the treated hemp fibers can be observed (Figure 1(c)). The surface of the treated hemp fibers is covered with particles smaller than 1 µm, as can be seen in Figure 1(d). These particles do not appear at the surface of raw hemp fibers (Figure 1 (b)). These results confirmed our previous statement about the plasticization of the middle lamella of hemp fibers which is mainly composed of lignin and extractives (*12,33*). The enzymatic treatment caused a partial defibrillation of the hemp fibers. Moreover, the small particles could correspond to extracted lignin. The lignin was removed from the middle lamella and dispersed in the water during the enzymatic treatment (*34,35*). Small particles of spherical lignin were then deposited at the surface of the fibers when the fibers
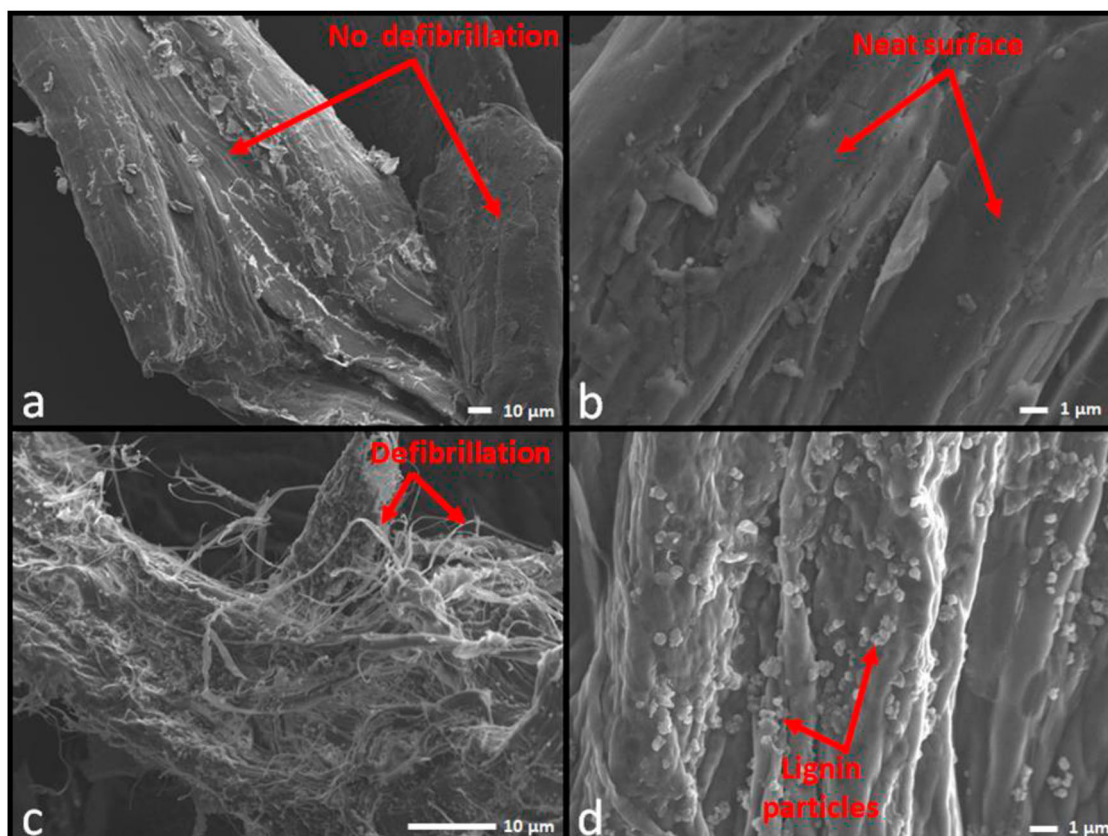
Figure 1. Surface analysis of raw hemp fibers (a, b) and enzymatically treated hemp fibers (c, d).

were filtered at the end of the treatment. The citrate/phosphate buffer could also induce soft acidic-mediated processes: acidic treatment commonly removes the extractives (e.g. pectin, resins, waxes) which is consistent with the yellowish color of the filtrate, (33) acidic treatment is also known to ease the decohesion of the fiber elements (12). The significant loss of mass during the pretreatment should be related to a large amount of the BDF used for the process, the removal of extractive, and the degradation or removal of lignin.

Mechanical characterizations and dispersion of the fibers

The tensile testing was conducted on each material reported in Table 1. The elongation at break was measured and the results are reported in Figure 2. The composites made of PLA showed no significant evolution of the elongation at break with the incorporation of non-treated or treated hemp fibers, even at 10 wt.% or 20 wt.%. The elongation at break of these composites is comprised of between $8 \pm 3\%$ (PLA-H10) and $10 \pm 0\%$ (both PLA-T10 and PLA-T20) while the reference of neat PLA was measured at $11 \pm 2\%$. The evolution of the elongation at break of the composites made of ePLA is much more significant because the reference of ePLA is close to $550 \pm 60\%$. This led to a series of composites with very different values for their elongation at break. ePLA-H10 and ePLA-H20 reached $380 \pm 80\%$ and $90 \pm 13\%$, respectively, while ePLA-T10 and ePLA-T20 broke at $230 \pm 60\%$ and $90 \pm 15\%$, respectively. The overall decrease in elongation at the break following the incorporation of lignocellulosic fibers (with or without any pretreatment) was often reported in the literature for polylactic acid or elastomer composites (13,36–38). A loss of cohesion in the material due to a poor surface adhesion between the matrix and the lignocellulosic fibers as well as fiber aggregates was often pointed out. In our study, one can also suggest a lack of adhesion between the BDF contained in the ePLA matrix and lignocellulosic fiber. As a hypothesis, the BDF used for the treatment of the fibers only acted as a plasticizer to increase the aspect ratio and was not grafted on the surface of the fibers. Moreover, it appears the results are better without treatment as ePLA-H10 has a better elongation at break than ePLA-T10 ($380 \pm 80\%$ vs $230 \pm 60\%$). Increasing the aspect ratio would logically increase the surface contact between the matrix and the fibers. Indeed, lowering the elongation at break is fully consistent with the increase in aspect ratio and a lack of adhesion between the matrix and the fibers.
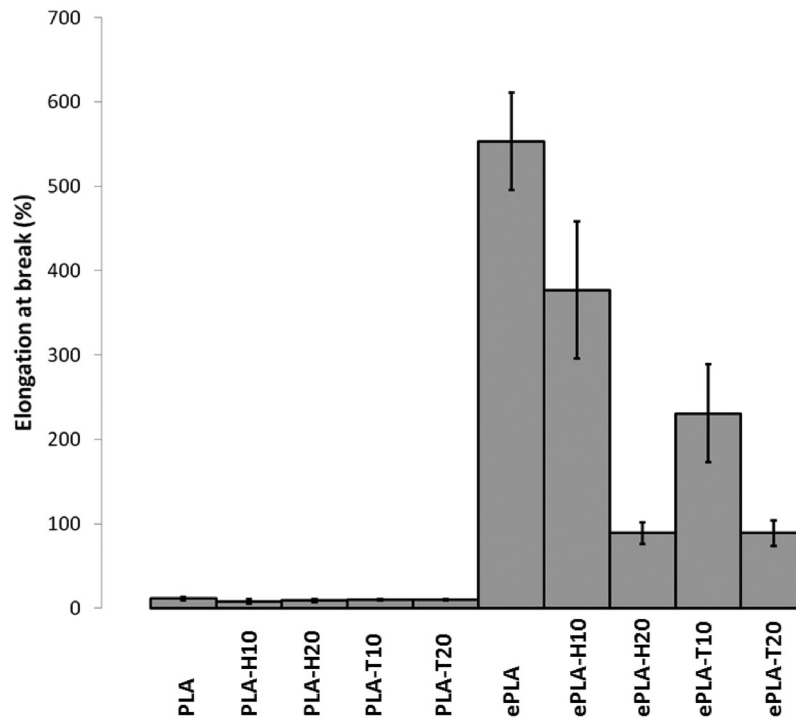
Figure 2. Elongation at the break of PLA and/or ePLA filled with non-treated or pretreated hemp fibers.

The interface between fibers and PLA as well as between fibers and ePLA was studied by SEM. The results are given in Figure 3. No significant differences in the distance and in the free volume between the polymeric matrix and the fibers can be observed in the composites. One can find more differences in the same composite than in different composites, meaning the experimental error of the characterization is very important (Figure 3(a,b)). Some fibrils can be observed for PLA-T20 and ePLA-T20 (Figure 3(b,d)). This is consistent with the defibrillation observed after the enzymatic treatment of the fibers (Figure 1). Figure 3(c,d) related to ePLA-H20 and ePLA-T20 composites show the presence of crystallites of BDF homogeneously dispersed in the PLA matrix. Such crystallites were observed in our previous works (39). These crystallites can also be found at the interface between the polymeric matrix and the fibers. There is a correlation between the presence of such BDF crystallites at the interface with the fibers and the decrease in the mechanical properties following the increase in the aspect ratio of the fibers which is consistent with our previous statement. One can suggest a physical mechanism in which the fibers are in contact with the BDF crystallites instead of the polymeric matrix. Indeed, there is more free volume between the fibers and the polymer when BDF crystallites are located at the interface (Figure 3(e,f)).

The dispersion of the fibers in the composites was studied by optical microscopy. The results are given in Figure 4. No significant differences in the dispersion of the fibers can be observed. The decreases in the mechanical properties of the composites are much more dependent on the interface between the fibers and the polymeric matrix than on the dispersion of the fibers.

As reported in Figure 5, the tensile strength of PLA containing fibers showed an increase from 81 ± 9 MPa (reference of PLA) to 82 ± 10 MPa (PLA-H10) and 98 ± 13 (PLA-H20), and to 94 ± 9 MPa (PLA-T10) and 103 ± 9 MPa (PLA-T20). The treatment of the fibers appears to slightly enhance the increase of the tensile strength observed after the incorporation of fibers in the PLA matrix. The tensile strength is not significantly modified after the incorporation of fibers in the ePLA matrix. Considering the margin of error, every material based on the ePLA matrix shows a value in the range of 19 ± 1 to 22 ± 1 MPa. This result is consistent with our previous statement about the poor surface adhesion between the ePLA matrix and fibers resulting in a loss of cohesion in the composites. It could also mean the surface adhesion between the PLA matrix and fibers appears to be better than between the ePLA matrix and fibers, even with or without pretreatment. The orientation of the fibers could also play a role (40). Our previous study in polycaprolactone (PCL) containing up to 22.5 wt.% of hemp fibers has shown the fibers in the core of the tensile test specimen were oriented following the longitudinal axis resulting from the injection process (41). As the injection process was the same, one
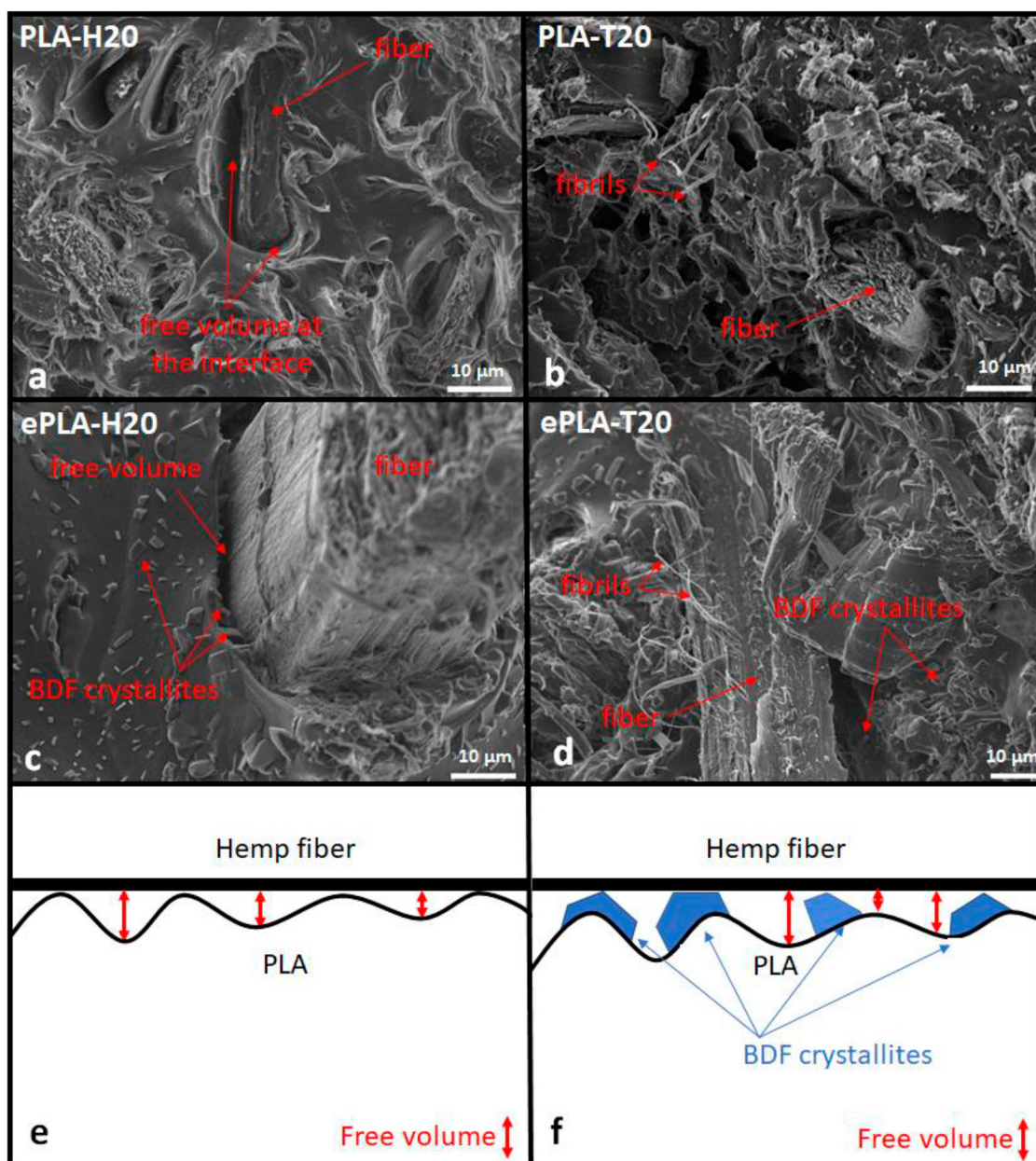
Figure 3. Interface analysis of PLA and/or ePLA filled with non-treated or pretreated hemp fibers.

can suggest a very analogous orientation of the fibers in the PLA-H and PLA-T composites.

An increase in Young's modulus was reported for PLA-H10 (2860 ± 160 MPa) and PLA-H20 (3300 ± 380 MPa), as well as for PLA-T10 (3300 ± 60 MPa) and PLA-T20 (3100 ± 260 MPa), in comparison with the reference of PLA (2490 ± 150 MPa), as reported in Figure 6. No trend emerges from these results due to the margin of error. An increase in stiffness is also commonly described in the literature for PLA containing treated or non-treated hemp fibers (42). Same overall trend is reported for ePLA containing fibers. There is an increase in Young's modulus from 38 ± 9 MPa (ePLA) to 180 ± 40 MPa (ePLA-H10) and 530 ± 120 (ePLA-H20). The use

of treated fibers also increased Young's modulus to 290 ± 40 MPa (ePLA-T10) and 590 ± 40 (ePLA-T20) in comparison with the neat ePLA matrix. The ePLA matrix appears to be of interest for the preparation of composites reinforced with natural fibers with a tunable compromise between elongation at break and stiffness. For such purposes, the use of non-treated hemp fibers appears to be more convenient and gives better results. Moreover, a comparison with values found in the literature demonstrates that ePLA reinforced with hemp fibers has an analog behavior to thermoplastic polyurethane (TPU) reinforced with hemp fibers (13). The decrease in Young's modulus with an increase in the elongation at break could make
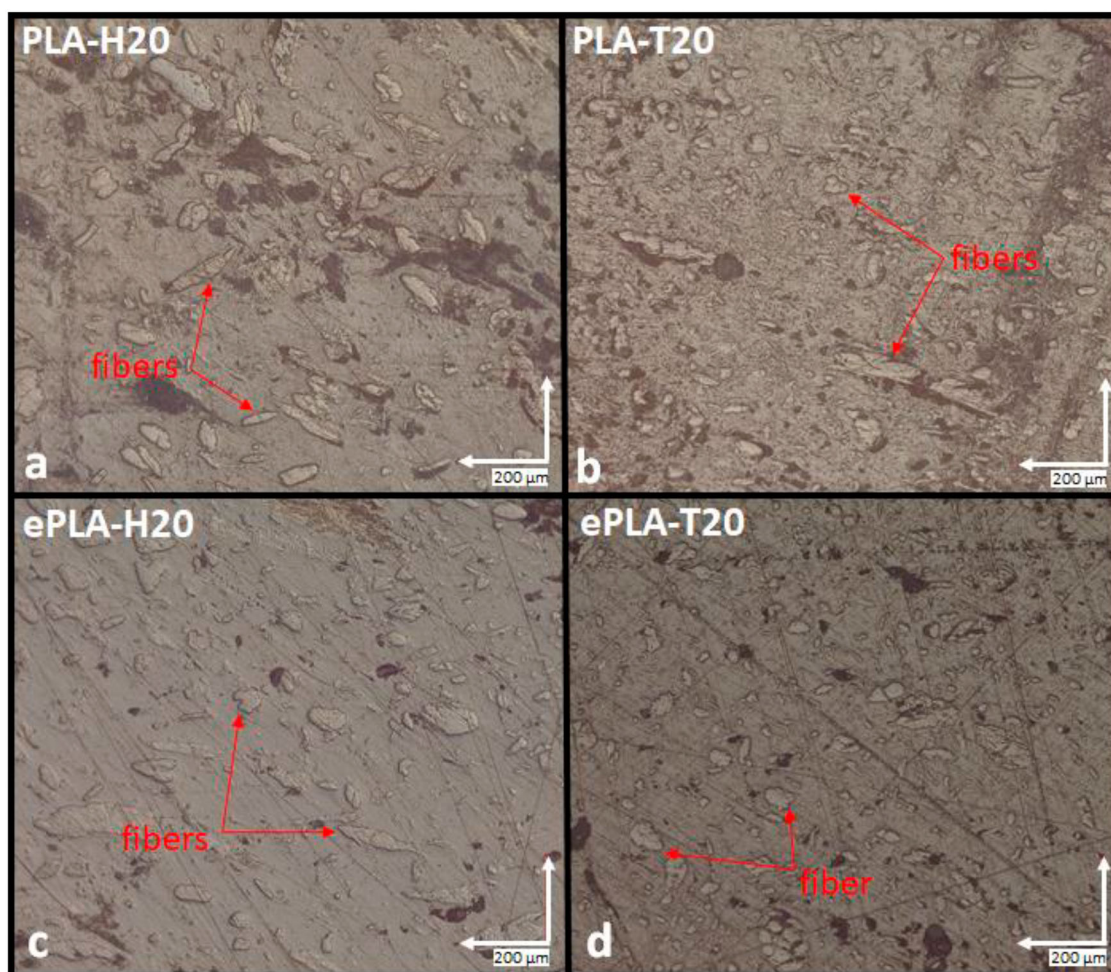
Figure 4. Dispersion of non-treated and pretreated hemp fibers in the PLA and ePLA matrix.

these composites suitable for the replacement of TPU in soft applications (e.g. coated fabrics, alternatives to leather). The decrease in Young's modulus in comparison with thermoplastic PLA could be a problem for rigid applications. As reported in the literature, the addition of other polymers (e.g. PBAT, PLGA) could help prepare such rigid composite with enhanced elongation at break (*43,44*). This could make these composites suitable to serve as more sustainable alternatives for oil-based composites currently used in rigid applications (e.g. transportation and building).

Thermal analysis

The crystalline fraction of PLA chains (χc) was comprised between 1.2% and 3.6% for the full set of materials (Table 2). The melting enthalpy of ePLA was too low to be significant and the crystalline fraction was arbitrarily considered to be lower than 1%. This overall crystalline fraction is too low to play a role in the mechanical properties quantified and discussed earlier in this study (*45*). This confirms that only the presence of hemp fibers in

the polymeric matrix plays a role in the evolution of the mechanical properties of our materials. No trend appears concerning the evolution of Tg regarding the incorporation of hemp fibers. The crystalline fraction of the material appears to be too low to be significant and its evolution is also inconsistent with the evolution of Tg. No correlation can be made at this stage between the mechanical properties and Tg. The Tg of ePLA explaining its elastomeric behavior at room temperature was already described elsewhere (*28*).

The residue observed at 500 °C for neat PLA is 0.8%, while the one for ePLA is 3.1%. This difference in a residual mass of 2.3% means the charring is more important for ePLA than for PLA (Table 2). One can suggest a synergistic effect between PLA and BDF during the thermal degradation of the blend. Neat PLA reinforced with non-treated hemp fibers exhibits a residue of 3.9% (PLA-H10) and 7.7% (PLA-H20), while it is 3.1% and 6.0% for PLA-T10 and PLA-T20, respectively. The residue increases with the fibers content which is following the analyses of the fibers where a higher residue was obtained for non-treated hemp fibers (29.3%) and
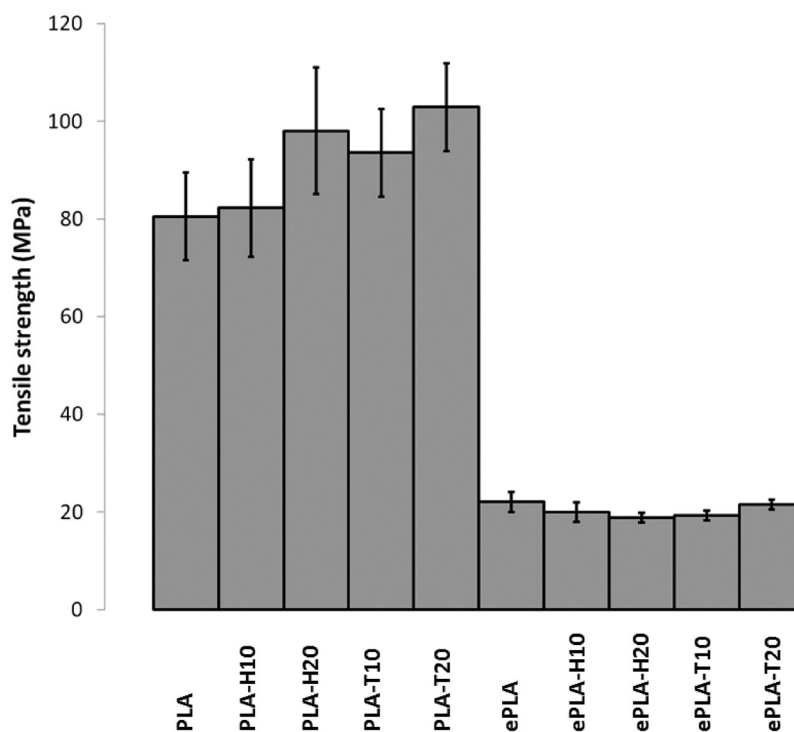
Figure 5. Tensile strength of PLA and/or ePLA filled with non-treated or pretreated hemp fibers.

treated hemp fibers (23.4%). A lower residue reported for treated hemp fibers in comparison with non-treated hemp fibers is consistent with the removal of lignin and extractives due to the enzymatic treatment as discussed previously (46). The residues quantified for ePLA-H10, ePLA-H20, ePLA-T10, and ePLA-T20 are 6.9%, 10.9%, 7.5%, and 8.9%, respectively. The overall trend is the same as the one reported for neat PLA composites. Moreover, it appears that the difference in residues between the ePLA composites and the PLA composites (for equivalent content and comparable treatment) is higher than the difference between the residue of ePLA and the residue of PLA. The difference in residual mass between ePLA-H10 and PLA-H10 is 3%, and between ePLA-H20 and PLA-H20 is 3.2%. This accounts for a possible synergistic effect between the fibers and BDF because the difference in residual mass in the composite containing both BDF and fibers in PLA versus the composite containing only fibers is higher than the difference in residual mass in a blend containing BDF in PLA (ePLA) versus raw PLA. The difference in residual mass between ePLA-T10 and PLA-10 is 4.4%, and between ePLA-T20 and PLA-T20 is 2.9%. This is in accordance with the previous statement related to a possible synergistic effect between BDF and fibers in PLA.

Linear combinations were calculated to determine the antagonistic and synergistic effects in the blends during thermal degradation using the data collected for raw materials (PLA, BDF, non-treated hemp fibers, and treated hemp fibers). The results are given in Figures 7–9. Destabilization effects are observed when treated or non-treated hemp fibers are incorporated into the blends meaning the combination of PLA and fibers, with or without BDF, reduced the thermal stability. Lower thermal stability of the fibers resulting in the production of decomposition products could explain this antagonistic effect where PLA degrades at a lower temperature. Indeed, non-treated and treated fibers start to degrade at 225 and 259 °C, respectively, while PLA starts its degradation at 334 °C (Table 2). These results also surprisingly indicated there is no interaction between BDF and fibers (treated or not) during the thermal degradation. Nevertheless, there is a significant synergistic effect between PLA and BDF after 375 °C leading to an increase in the charring and of the final residue (Figure 9).

Reaction to fire

The reaction to fire of the materials was evaluated using mass loss cone calorimetry to measure the Heat Release Rate (HRR) during the combustion. The results are shown in Figures 10 and 11. Pictures of the residues after the experiments are given in Figure 12. The mean Peak of Heat Release Rate (pHRR) of the three PLA plates is 342 kW.m-2 and the Total Heat Release (THR) of PLA is 75.6 MW.m-2. PLA left no measurable charring residue.
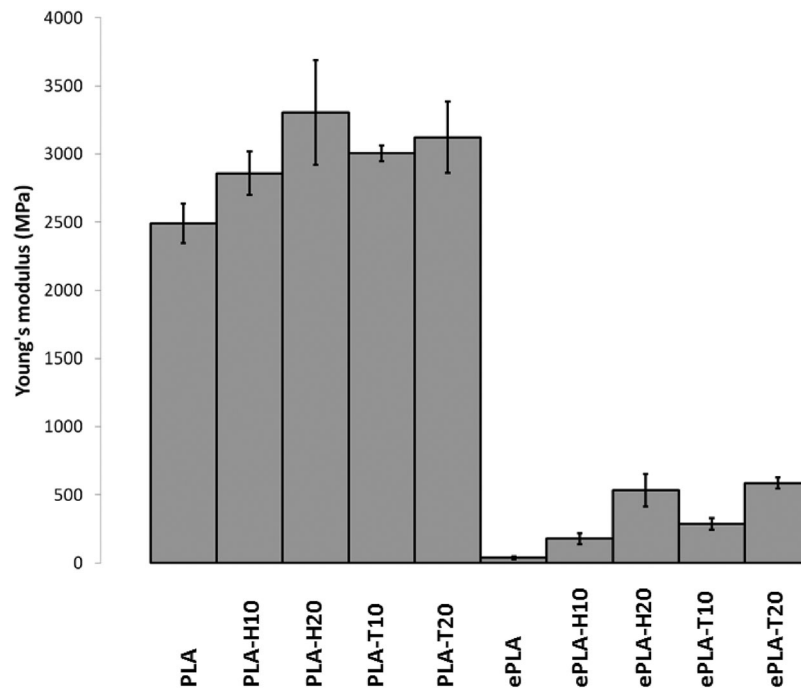
Figure 6. Young's modulus of PLA and/or ePLA filled with non-treated or pretreated hemp fibers.

These data will serve as references to evaluate the reaction to fire of the composites.

The mean pHRR of PLA-H20 is 344 kW.m-2 and that of PLA-T20 is 329 kW.m-2. The mean charring residue left by PLA-H20 is 2 wt.% and that left by PLA-T20 is less than 1 wt.%. The mean THR of PLA-H20 is 76.0 MW.m-2 and that of PLA-T20 is 80.4 MW.m-2. There is no significant difference between the pHRR of PLA-H20 and PLA-T20 in comparison with the pHRR of PLA. The incorporation of 20 wt.% of raw hemp fibers or enzymatically treated hemp fibers in PLA did not change the reaction to fire excepting a notable reduction of the ignition time down to 50 s (Figure 10). The combustion of the composites left a small amount of residue. The differences in THR between the composites and the PLA reference are not significant. These results are consistent with the literature where the incorporation of natural fibers in PLA led to no significant effect on the reaction to fire (47).

The mean pHRR of ePLA, ePLA-H20, and ePLA-T20 is overall 10% higher than the mean pHRR of PLA (respectively 361, 376, and 372 kW.m^{-2} vs 342 kW.m^{-2}) which is in the margin error. The mean charring residue left by ePLA, ePLA-H20, and ePLA-T20 is respectively 3wt.%, 7wt.%, and 2wt.%. The THR of ePLA is 12% lower than that of PLA, and the THR of ePLA-H20 is 14% lower. The THR of ePLA-T20 is 5% higher than that of PLA. The difference in pHRR between ePLA and the PLA reference is not very important but one can consider it significant. There is a minor degradation of the reaction to fire due to the presence of BDF in the material. This could be explained by chemical interactions between the PLA matrix, the BDF, and their respective degradation products. Lactide oligomers, lactic acid, acetaldehyde, carbon monoxide/

Table 2. Thermal properties of fibers, BDF, PLA and/or ePLA reinforced with non-treated or pretreated hemp fibers.

| Materials	Tg (°C, ± 1) (thermal history erased)	Tm (°C)	χ (%, ± 3) (thermal history)	T5 (°C)	Tdmax (°C)	Residue at 500 °C (%)
Non-treated hemp fibers	–	–	–	225	316	29.3
Treated hemp fibers	–	–	–	259	352	23.4
BDF	−19.1	106	100	206	348	0.5
PLA	56.0	140.1	1.2	334	373	0.8
PLA-H10	53.1	138.2	1.8	291	338	3.9
PLA-H20	58.1	140.9	1.3	276	317	7.7
PLA-T10	54.4	138.7	2.3	305	350	3.1
PLA-T20	52.8	137.2	2.8	287	331	6.0
ePLA	18.7	129.3	≤1	299	356	3.1
ePLA-H10	15.7	125.0	1.9	268	304–341	6.9
ePLA-H20	16.7	119.9	1.9	263	302–334	10.6
ePLA-T10	18.8	126.1	3.6	275	320–353	7.5
ePLA-T20	17.4	123.9	3.5	271	5309–346	8.9
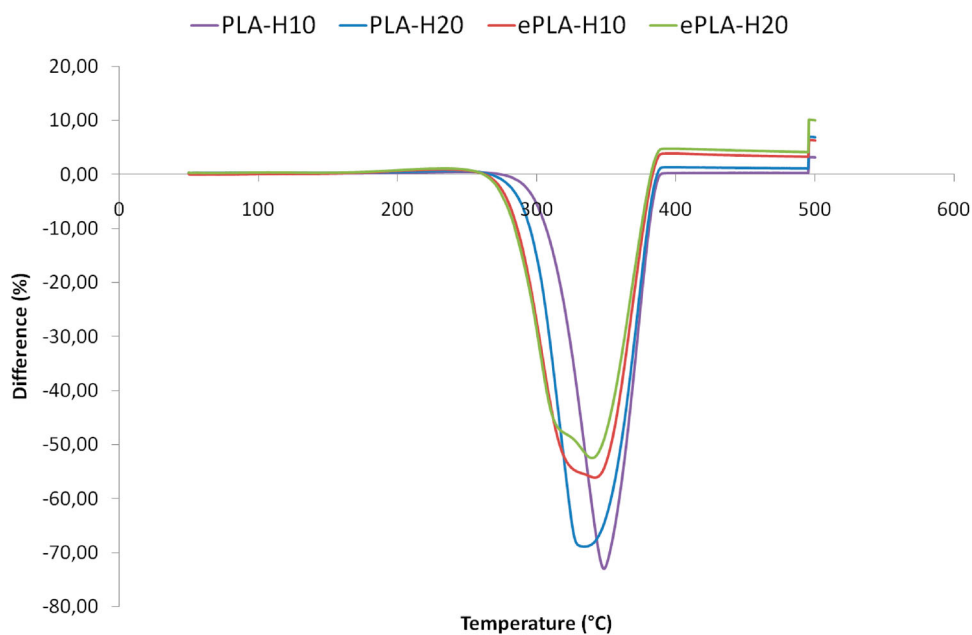
Figure 7. Difference between the linear combination of thermogravimetric analyses between PLA, BDF, and non-treated hemp fibers, and thermogravimetric analyses of their respective blends.

dioxide, and water are produced during the thermal degradation of PLA (*48,49*). The water and the lactic acid produced during the degradation of PLA would help the hydrolysis of BDF into ferulic acid and could lead to the formation of guaiacol and guaiacol derivatives (mainly 4-methylguaiacol, 4-ethylguaiacol, and 4-vinyl-guaiacol after the thermal degradation of ferulic acid (*50*). An analog trend is observed for ePLA-H20 in comparison with PLA-H20. The interaction between BDF and

hemp fibers appears to be an antagonistic effect increasing the pHRR. Nevertheless, it is interesting to note an increase in the charring residue going from almost nothing (PLA) to 3wt.% (ePLA) and from 2wt.% (PLA-H20) to 7wt.% (ePLA-H20). It is consistent with our previous statement from thermal analysis where a synergistic effect was noted between BDF and fibers increasing the residue. This charring effect is not sufficient to improve the reaction to fire of PLA containing both hemp fibers
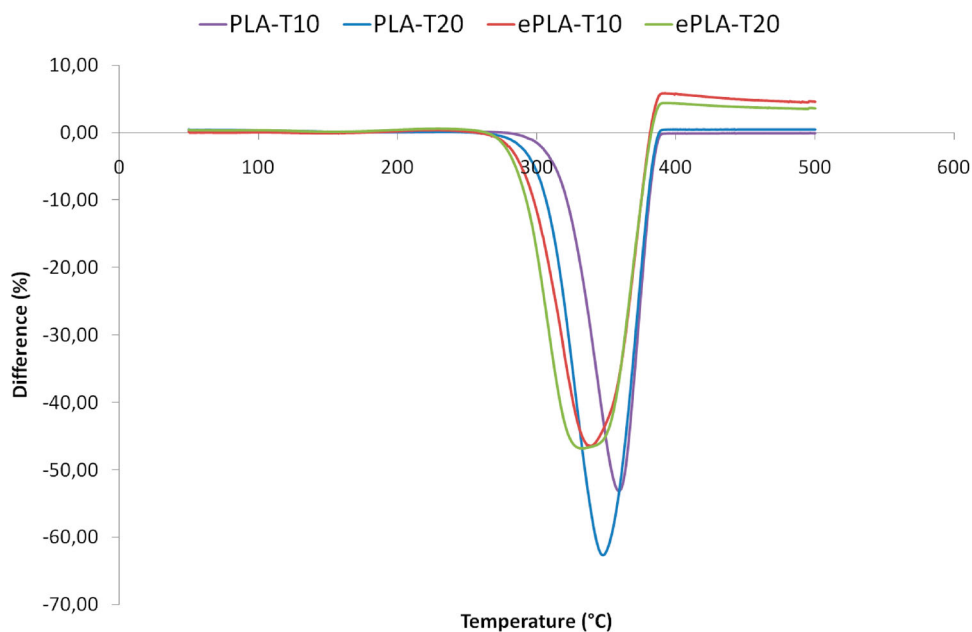
Figure 8. Difference between the linear combination of thermogravimetric analyses between PLA, BDF, and treated hemp fibers, and thermogravimetric analyses of their respective blends.
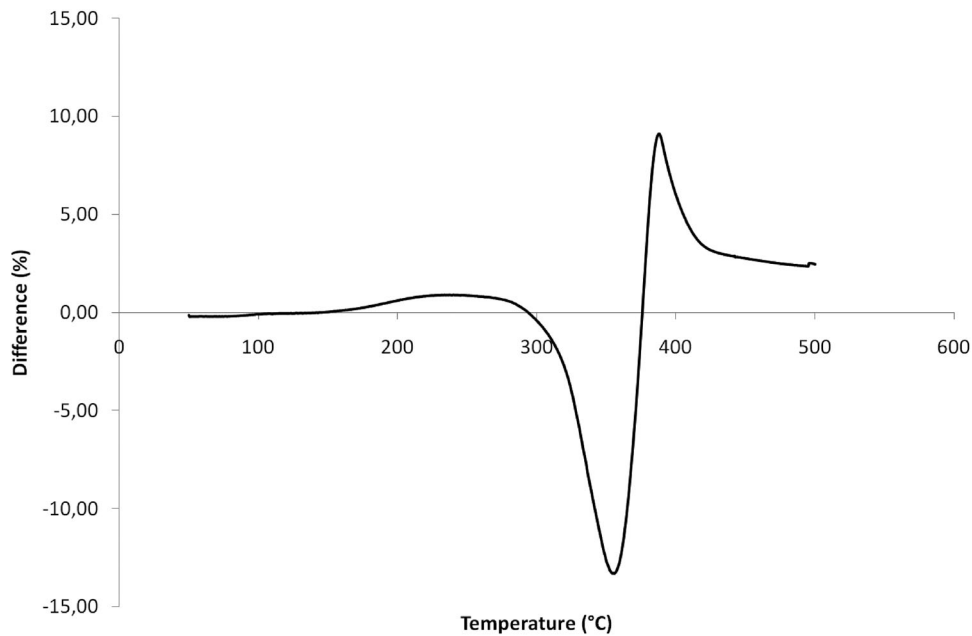
Figure 9. Difference between the linear combination of thermogravimetric analyses between PLA and BDF and thermogravimetric analysis of their blends.

and BDF, but it could be useful in combination with flame retardants (FR). Literature reports several natural fibers treated with FR exhibiting improved flammability that could be used in combination with BDF (*47*). Moreover, the use of nanoparticles could also be of interest to improve fire performance as the literature reports (*51*).

Moreover, ePLA-T20 exhibits the worst flammability results since its pHRR is close to that of ePLA-H20 (respectively, 372 and 376 kW.m^{-2}) but its THR is the biggest (+5% for ePLA-T20 in comparison with PLA, while it is −14% for ePLA-H20) and its charring residue is only 2wt.%. It could be very consistent with the removal of lignin and extractives due to the enzymatic treatment as lignin improve the flame retardancy of PLA (*52*). One can suggest that the chemical interactions between BDF and hemp fibers during the thermal degradation leading to an increase in the charring residue could involve lignin and extractives.
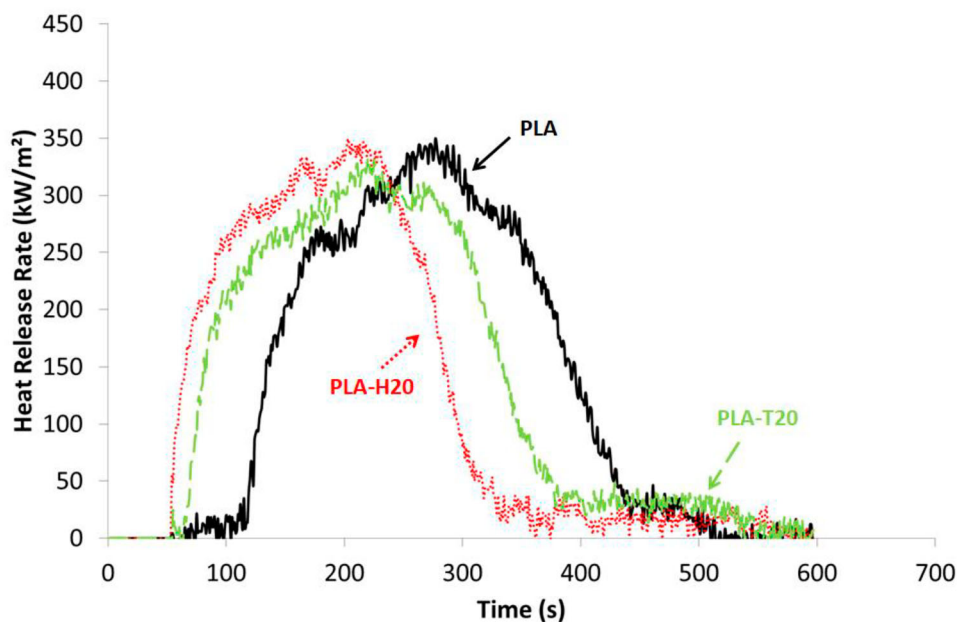
Figure 10. Heat release rates of PLA, PLA-H20, and PLA-T20.
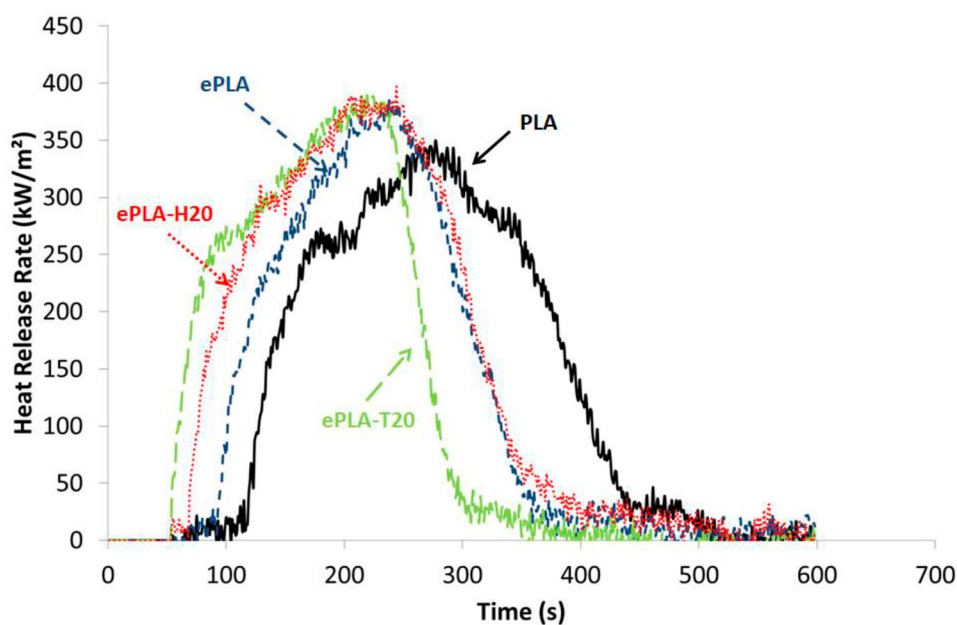
Figure 11. Heat release rates of PLA, ePLA, ePLA-H20s and ePLA-T20.
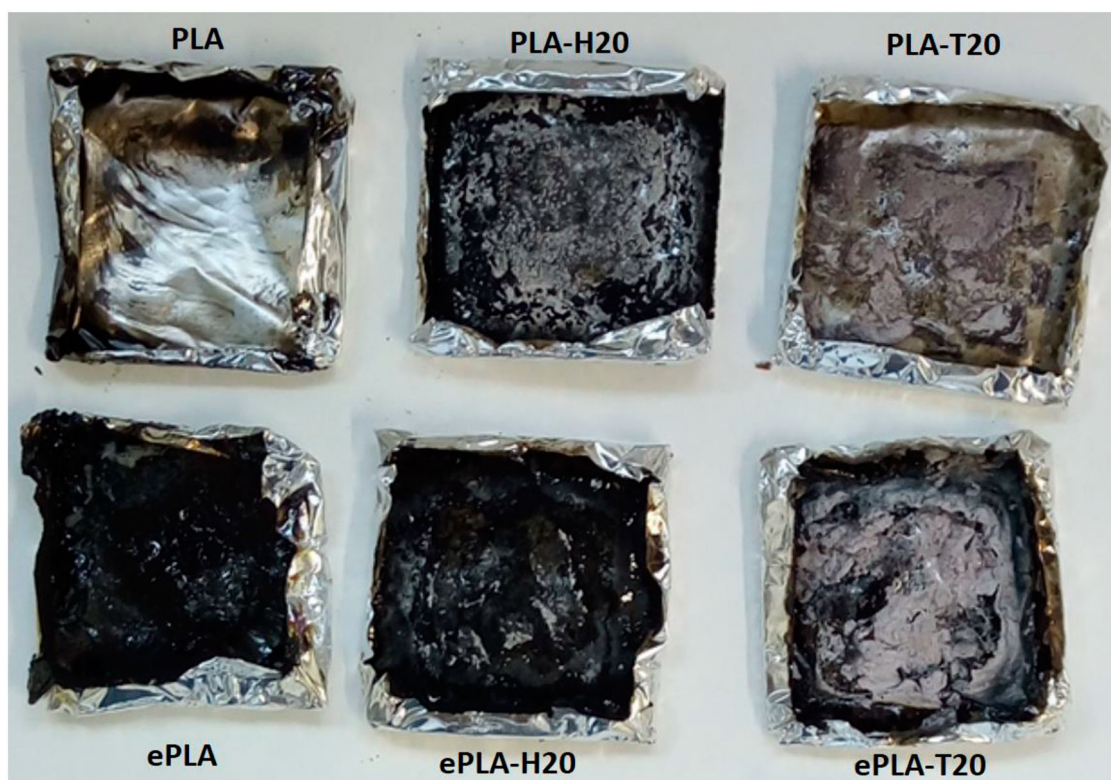
Figure 12. Charring residues resulting from the fire testing experiments conducted on composites.

Conclusion

In light of the results described in this study and, in comparison with other elastomers such as thermoplastic polyurethane (TPU) reinforced with natural fibers, it appears that composites made of elastomeric PLA (ePLA) and hemp fibers are of interest for the preparation of fully bio-based composites with tunable mechanical properties. The ePLA matrix is suitable for the preparation of composites reinforced with natural fibers with a compromise between elongation at break

and stiffness. The use of ferulic acid derivative has no significant impact on the dispersion of the fibers. Crystallites of ferulic acid derivative were found homogenously dispersed in the PLA and some of them were found at the interface between the fibers and the PLA. There is a correlation between the decrease in the mechanical properties following the increase of the aspect ratio of the fibers and the presence of such crystallites at the interface.

The enzymatic treatment of the fibers did not achieve to graft ferulic acid derivative at their surface. A defibrillation of the fibers was observed. A removal of extractives and lignin from the fibers due to the enzymatic treatment is suspected. Moreover, the ePLA matrix showed a slightly degraded reaction to fire in comparison with raw PLA and exhibited a charring residue meaning that elastomeric PLA could be suitable to be used in combination with intumescent conventional flame retardant (e.g. phosphates) and/or nanoparticles (e.g. nanoclays). A synergistic effect between the hemp fibers and the BDF increased the charring residue. A chemical interaction between BDF and lignin is suspected. The removal of the lignin from the fibers due to the enzymatic treatment is correlated to the degradation of the reaction to fire of the composites.

Acknowledgements

Disclosure statement

Antoine Gallos and Florent Allais are the inventors of the patent #Shape memory polymers based on poly(hydroxy alkanoates) WO2020165075 issued to AgroParisTech.

Funding

References

[1] Ramesh, M.; Palanikumar, K.; Reddy, K.H. Plant Fibre Based bio-Composites: Sustainable and Renewable Green Materials. *Renew. Sustain. Energy Rev.* **2017,** *79,* 558–84. doi:10.1016/j.rser.2017.05.094.

[2] Mathes, V. The Composites Industry: Plenty of Opportunities in Heterogeneous Market. *Reinf. Plast.* **2018,** *62,* 44–51. doi:10.1016/j.repl.2017.05.002.

[3] AL-Oqla, F.M.; Sapuan, S.M.; Ishak, M.R.; Nuraini, A.A. Predicting the Potential of Agro Waste Fibers for Sustainable Automotive Industry Using a Decision Making Model. *Comput. Electron. Agric.* **2015,** *113,* 116–27. doi:10.1016/j.compag.2015.01.011.

[4] Bhoopathi, R.; Ramesh, M. Influence of Eggshell Nanoparticles and Effect of Alkalization on Characterization of Industrial Hemp Fibre Reinforced Epoxy Composites. *J. Polym. Environ.* **2020,** *28,* 2178–90. doi:10.1007/s10924-020-01756-1.

[5] Kim, N.K.; Dutta, S.; Bhattacharyya, D. A Review of Flammability of Natural Fibre Reinforced Polymeric Composites. *Compos. Sci. Technol.* **2018,** *162,* 64–78. doi:10.1016/j.compscitech.2018.04.016.

[6] Ramesh, M.; Deepa, C.; Kumar, L.R.; Sanjay, M.; Siengchin, S. Life-cycle and Environmental Impact Assessments on Processing of Plant Fibres and its bio-Composites: A Critical Review. *J. Ind. Text.* **2022,** *51,* 5518S–5542S. doi:10.1177/1528083720924730.

[7] Vink, E.T.H.; Davies, S. Life Cycle Inventory and Impact Assessment Data for 2014 Ingeo™Polylactide Production. *Indus. Biotechnol.* **2015,** *11,* 167–80. doi:10.1089/ind.2015.0003.

[8] Niaounakis, M. Recycling of Biopolymers – The Patent Perspective. *Eur. Polym. J.* **2019,** *114,* 464–75. doi:10.1016/j.eurpolymj.2019.02.027.

[9] Botvin, V.; Karaseva, S.; Khasanov, V. Depolymerization of Lactic Acid Oligomers Into Lactide: Epimerization, Stereocomplex Formation, and Nature of Interactions of Oligomers. *Polym. Degrad. Stab.* **2020,** *182,* 109382. doi:10.1016/j.polymdegradstab.2020.109382.

[10] Siakeng, R.; Jawaid, M.; Ariffin, H.; Sapuan, S.M.; Asim, M.; Saba, N. Natural Fiber Reinforced Polylactic Acid Composites: A Review. *Polym. Compos.* **2019,** *40,* 446–63. doi:10.1002/pc.24747.

[11] González-López, M.E.; Robledo-Ortíz, J.R.; Manríquez-González, R.; Silva-Guzmán, J.A.; Pérez-Fonseca, A.A. Polylactic Acid Functionalization with Maleic Anhydride and its use as Coupling Agent in Natural Fiber Biocomposites: A Review. *Compos. Interfaces* **2018,** *25,* 515–38. doi:10.1080/09276440.2018.1439622.

[12] Gallos, A.; Paës, G.; Allais, F.; Beaugrand, J. Lignocellulosic Fibers: A Critical Review of the Extrusion Process for Enhancement of the Properties of Natural Fiber Composites. *RSC Adv.* **2017**, *7,* 34638–54. doi:10.1039/C7RA05240E.

[13] Haghighatnia, T.; Abbasian, A.; Morshedian, J. Hemp Fiber Reinforced Thermoplastic Polyurethane Composite: An Investigation in Mechanical Properties. *Ind. Crops Prod.* **2017,** *108,* 853–63. doi:10.1016/j.indcrop.2017.07.020.

[14] Alias, N.F.; Ismail, H. An Overview of Toughening Polylactic Acid by an Elastomer. *Polym. Plast. Technol.*

Mater. **2019,** *58*, 1399–422. doi:10.1080/25740881.2018.1563118.

[15] Jašo, V.; Cvetinov, M.; Rakić, S.; Petrović, Z.S. Bio-plastics and Elastomers From Polylactic Acid/Thermoplastic Polyurethane Blends. *J. Appl. Polym. Sci.* **2014,** *131*. doi:10.1002/app.41104.

[16] Jing, X.; Mi, H.-Y.; Peng, X.-F.; Turng, L.-S. The Morphology, Properties, and Shape Memory Behavior of Polylactic Acid/Thermoplastic Polyurethane Blends. *Polym. Eng. Sci.* **2015,** *55*, 70–80. doi:10.1002/pen.23873.

[17] Mi, H.-Y.; Salick, M.R.; Jing, X.; Jacques, B.R.; Crone, W.C.; Peng, X.-F., Turng, L.-S.. Characterization of Thermoplastic Polyurethane/Polylactic Acid (TPU/PLA) Tissue Engineering Scaffolds Fabricated by Microcellular Injection Molding. *Mater. Sci. Eng. C* **2013**, *33*, 4767–76. doi:10.1016/j.msec.2013.07.037.

[18] Lai, S.-M.; Lan, Y.-C. Shape Memory Properties of Melt-Blended Polylactic Acid (PLA)/Thermoplastic Polyurethane (TPU) bio-Based Blends. *J. Polym. Res.* **2013,** *20*, 140. doi:10.1007/s10965-013-0140-6.

[19] Jašo, V.; Glenn, G.; Klamczynski, A.; Petrović, Z.S. Biodegradability Study of Polylactic Acid/Thermoplastic Polyurethane Blends. *Polym. Test.* **2015,** *47*, 1–3. doi:10.1016/j.polymertesting.2015.07.011.

[20] Tessier, S.; Fleury, M.; Roche, S. Overview of the Polyurethane Market and Technical State of the Art. *ADEME* **2014**, 1–106. (French)

[21] Simón, D.; Borreguero, A.M.; de Lucas, A.; Rodríguez, J.F. Recycling of Polyurethanes From Laboratory to Industry, a Journey Towards the Sustainability. *Waste Manage.* **2018,** *76*, 147–71. doi:10.1016/j.wasman.2018.03.041.

[22] Pandey, K.; Antil, R.; Saha, S.; Jacob, J.; Balavairavan, B. Poly(Lactic Acid)/Thermoplastic Polyurethane/Wood Flour Composites: Evaluation of Morphology, Thermal, Mechanical and Biodegradation Properties. *Mater. Res. Express* **2019,** *6*, 125306. doi:10.1088/2053-1591/ab5398.

[23] Jones, M.; Gandia, A.; John, S.; Bismarck, A. Leather-Like Material Biofabrication Using Fungi. *Nat. Sustain.* **2021,** *4*, 9–16. doi:10.1038/s41893-020-00606-1.

[24] Manaia, J.P.; Manaia, A.T.; Rodriges, L. Industrial Hemp Fibers: An Overview. *Fibers* **2019,** *7*, 106. doi:10.3390/fib7120106.

[25] Koohestani, B.; Darban, A.K.; Mokhtari, P.; Yilmaz, E.; Darezereshki, E. Comparison of Different Natural Fiber Treatments: A Literature Review. *Int. J. Environ. Sci. Technol.* **2019,** *16*, 629–42. doi:10.1007/s13762-018-1890-9.

[26] Morin, S.; Bockstal, L.; Jacquet, N.; Richel, A. One-Step Enzymatic Grafting of Ferulic Acid With Cellulose to Enhance Matrices–Fibres Compatibility in Bio-Composites. *J. Mater. Sci.* **2019,** *54*, 13314–21. doi:10.1007/s10853-019-03832-x.

[27] Gallos, A.; Allais, F. Shape Memory Polymers Based on Poly(Hydroxyalkanoates). *WO2020165075* **2020**.

[28] Gallos, A.; Crowet, J.-M.; Michely, L.; Raghuwanshi, V.S.; Mention, M.M., Langlois, V. Blending Ferulic Acid Derivatives and Polylactic Acid Into Biobased and Transparent Elastomeric Materials with Shape Memory Properties. *Biomacromolecules* **2021**. doi:10.1021/acs.biomac.1c00002.

[29] Kasmi, S.; Gallos, A.; Beaugrand, J.; Paës, G.; Allais, F. Ferulic Acid Derivatives Used as Biobased Powders for a

Convenient Plasticization of Polylactic Acid in Continuous Hot-Melt Process. *Eur. Polym. J.* **2019,** *110*, 293–300. doi:10.1016/j.eurpolymj.2018.11.036.

[30] Reano, A.F.; Pion, F.; Domenek, S.; Ducrot, P.H.; Allais, F. Chemo-Enzymatic Preparation and Characterization of Renewable Oligomers With Bisguaiacol Moieties: Promising Sustainable Antiradical/Antioxidant Additives. *Green Chem.* **2016**, *18*, 3334–45. doi:10.1039/C6GC00117C.

[31] Allais, F.; Pion, F.; Reano, A.F.; Ducrot, P.-H.; Spinner, H.E. Phenol Polymer with 5,5'-Biaryl Bonds, Methods for Preparing Same, and Uses Thereof. *WO2015055936* **2015**.

[32] Janvier, M.; Hollande, L.; Jaufurally, A.S.; Pernes, M.; Ménard, R., Grimaldi, M.. Syringaresinol: A Renewable and Safer Alternative to Bisphenol A for Epoxy-Amine Resins. *ChemSusChem.* **2017,** *10*, 738–46. doi:10.1002/cssc.201601595.

[33] Yang, J.; Ching, Y.; Chuah, C. Applications of Lignocellulosic Fibers and Lignin in Bioplastics: A Review. *Polymers* **2019,** *11*, 751. doi:10.3390/polym11050751.

[34] Österberg, M.; Sipponen, M.H.; Mattos, B.D.; Rojas, O.J. Spherical Lignin Particles: A Review on Their Sustainability and Applications. *Green Chem.* **2020,** *22*, 2712–33. doi:10.1039/D0GC00096E.

[35] Mičić, M.; Jeremič, M.; Radotič, K.; Mavers, M.; Leblanc, R.M. Visualization of Artificial Lignin Supramolecular Structures. *Scanning* **2000,** *22*, 288–94. doi:10.1002/sca.4950220503.

[36] Miedzianowska, J.; Masłowski, M.; Strzelec, K. Thermoplastic Elastomer Biocomposites Filled with Cereal Straw Fibers Obtained with Different Processing Methods—Preparation and Properties. *Polymers* **2019,** *11*, 641. doi:10.3390/polym11040641.

[37] Zhang, Q.; Shi, L.; Nie, J.; Wang, H.; Yang, D. Study on Poly (Lactic Acid)/Natural Fibers Composites. *J. Appl. Polym. Sci.* **2012,** *125*, E526–33. doi:10.1002/app.36852.

[38] Smitthipong, W.; Suethao, S.; Shah, D.; Vollrath, F. Interesting Green Elastomeric Composites: Silk Textile Reinforced Natural Rubber. *Polym. Test.* **2016,** *55*, 17–24. doi:10.1016/j.polymertesting.2016.08.007.

[39] Singh Raghuwanshi, V.; Gallos, A.; Joram Mendoza, D.; Lin, M.; Allais, F.; Garnier, G. Nanocrystallisation and Self-Assembly of Biosourced Ferulic Acid Derivative in Polylactic Acid Elastomeric Blends. *J. Colloid Interface Sci.* **2022**. doi:10.1016/j.jcis.2021.08.123.

[40] Mukherjee, T.; Kao, N. PLA Based Biopolymer Reinforced with Natural Fibre: A Review. *J. Polym. Environ.* **2011,** *19*, 714–25. doi:10.1007/s10924-011-0320-6.

[41] Gallos, A.; Paës, G.; Legland, D.; Allais, F.; Beaugrand, J. Exploring the Microstructure of Natural Fibre Composites by Confocal Raman Imaging and Image Analysis. *Compos. Part A Appl. Sci. Manuf.* **2017,** *94*, 32–40. doi:10.1016/j.compositesa.2016.12.005.

[42] Sawpan, M.A.; Pickering, K.L.; Fernyhough, A. Improvement of Mechanical Performance of Industrial Hemp Fibre Reinforced Polylactide Biocomposites. *Compos. Part A Appl. Sci. Manuf.* **2011,** *42*, 310–9. doi:10.1016/j.compositesa.2010.12.004.

[43] Kimble, L.D.; Bhattacharyya, D.; Fakirov, S. Biodegradable Microfibrillar Polymer-Polymer Composites From Poly(L-Lactic Acid)/Poly(Glycolic Acid). *Express. Polym. Lett.* **2015,** *9*, 300–7. doi:10.3144/expresspolymlett.2015.27.

[44] Kimble, L.D.; Bhattacharyya, D. *In Vitro* Degradation Effects on Strength, Stiffness, and Creep of PLLA/PBS: A Potential Stent Material. *Int. J. Polym. Mater. Polym. Biomater.* **2015**, *64*, 299–310. doi:10.1080/00914037.2014.945203.

[45] Orue, A.; Eceiza, A.; Arbelaiz, A. The Effect of Sisal Fiber Surface Treatments, Plasticizer Addition and Annealing Process on the Crystallization and the Thermo-Mechanical Properties of Poly(Lactic Acid) Composites. *Ind. Crops Prod.* **2018,** *118*, 321–33. doi:10.1016/j.indcrop.2018.03.068.

[46] Oza, S.; Ning, H.; Ferguson, I.; Lu, N. Effect of Surface Treatment on Thermal Stability of the Hemp-PLA Composites: Correlation of Activation Energy with Thermal Degradation. *Compos. Part B Eng.* **2014,** *67*, 227–32. doi:10.1016/j.compositesb.2014.06.033.

[47] Mngomezulu, M.E.; John, M.J.; Jacobs, V.; Luyt, A.S. Review on Flammability of Biofibres and Biocomposites. *Carbohydr. Polym.* **2014,** *111*, 149–82. doi:10.1016/j.carbpol.2014.03.071.

[48] Wachsen, O.; Reichert, K.H.; Krüger, R.P.; Much, H.; Schulz, G. Thermal Decomposition of Biodegradable Polyesters-III. Studies on the Mechanisms of Thermal Degradation of Oligo-l-Lactide Using SEC, LACCC and MALDI-TOF-MS. *Polym. Degrad. Stab.* **1997,** *55*, 225–31. doi:10.1016/S0141-3910(96)00127-9.

[49] McNeill, I.C.; Leiper, H.A. Degradation Studies of Some Polyesters and Polycarbonates-1. Polylactide: General Features of the Degradation Under Programmed Heating Conditions. *Polym. Degrad. Stab.* **1985,** *11*, 267–85. doi:10.1016/0141-3910(85)90050-3.

[50] Fiddler, W.; Parker, W.E.; Wasserman, A.E.; Doerr, R.C. Thermal Decomposition of Ferulic Acid. *J. Agric. Food Chem.* **1967,** *15*, 757–61. doi:10.1021/jf60153a003.

[51] Bourbigot, S.; Duquesne, S.; Fontaine, G.; Bellayer, S.; Turf, T.; Samyn, F. Characterization and Reaction to Fire of Polymer Nanocomposites with and Without Conventional Flame Retardants. *Mol. Cryst. Liq. Cryst.* **2008**, *486*, 325–339. doi:10.1080/15421400801921983.

[52] Costes, L.; Laoutid, F.; Aguedo, M.; Richel, A.; Brohez, S.; Delvosalle, C., Dubois, P., Phosphorus and Nitrogen Derivatization as Efficient Route for Improvement of Lignin Flame Retardant Action in PLA. *Eur. Polym. J.* **2016**, *84*, 652–67. doi:10.1016/j.eurpolymj.2016.10.003.